IJCRT.ORG ISSN : 2320-2882

INTERNATIONAL JOURNAL OF CREATIVE RESEARCH THOUGHTS (IJCRT)

An International Open Access, Peer-reviewed, Refereed Journal

Comparative Study of Structural Poisson's ratio and Natural Frequencies of a Nylon plate using Micro - polar elasticity theory and Classical Elasticity Theory

Saravanan Natarajan

Senior Lecturer

Engineering Department, MIE Section.

University of Technology and Applied Sciences (UTAS) , College of Engineering and Technology Muscat, Sultanate of Oman

Abstract: The main objective of this paper is, the finite element analysis of rectangular plate using Micropolar Elasticity Theory proposed by A.C. Eringen. A rectangular plate subjected to simple tensile loading was analyzed for different types of nylon materials (both glass filled and carbon filled) which are commercially available in market. A two-dimensional triangular finite element formulation including an extra degree of freedom at each node was derived based on the Eringen's Micropolar theory.The structural Poisson's ratio of nylon plate using Classical Elasticity theory were validated using results obtained using ANSYS software. A study on dynamic characteristics of plate had also been done using both the theories and results were compared.

Keywords: Micropolar Elasticity Theory; Classical Elasticity Theory; Structural Poisson's ratio; Finite element; Nylon; Modal Analysis.

I. INTRODUCTION

A. Cemel Eringen and his colleagues established the theory of micromorphic materials [1-3], which addresses a class of materials exhibiting specific microscopic effects resulting from the local structure and micro movements of the media. These materials are affected by spin inertia and can sustain stress and body moments. However, the general theory is extremely complex, and the differential equations are difficult to solve even in the case of linear elastic substances. Eringen presented a theory of pair stress in an attempt to simplify the complexity. Subsequently, "Micropolar Elasticity Theory" (MET) was used to replace this hypothesis.Unlike the pair stress theory, in micropolar elasticity the motion of the medium is fully specified and all components of the asymmetric stress tensor.

A material will often experience lateral contraction when subjected to tensile loading, whereas lateral elongation occurs when a compressive force is applied. The negative value of the ratio of lateral strain to longitudinal strain, when a uniaxial load is applied along its longitudinal direction, is known as the structural Poisson's ratio. As a result, Poisson's ratio is positive in the majority of isotropic elastic materials and has an admissible range of -1 to +.5 [4]. If a material experiences lateral contraction under compressive loading and lateral expansion under tensile loading, it is said to have a negative structural Poisson's ratio. These days, isotropic foam constructions with negative structural Poisson's ratio are being produced. Comparing these materials to conventional foam materials with positive Poisson's ratio, it is discovered that they have improved strength, impact absorption, strain fracture toughness, resilience, and shear modulus [6].

In this work, a suitable MATLAB computer program for solving a rectangular plate problem is built. A 2D triangle element with three nodes, each having an extra degree of freedom, is derived using MET and finite element methods. Both for Classical Elasticity Theory and Micropolar Elasticity Theory, the Structural Poisson's ratio of the rectangular plate is determined by selecting different glass-filled nylon materials that are commercially accessible. Both theories are used to study the variability in strains for various materials. Additionally, the investigation focuses on how the structural Poisson's ratio varies for various materials. For a variety of nylon material families, modal analysis (un-damped free vibration) was also carried out on the plate, and the associated natural frequencies were ascertained using both theories.

2. 2D-Micropolar Elasticity Theory:

2.1. 2D Micropolar Elasticity Theory:

The constitutive equations and the strain displacement relations for micropolar elasticiy theory are as follows:

$$t_{ij} = \lambda \varepsilon_{kk} \delta_{ij} + (\mu^* + k)\varepsilon_{ij} + \mu^* \varepsilon_{ji} \quad (1)$$

$$m_{ij} = \alpha \phi_{k,k} \delta_{ij} + \beta \phi_{i,j} + \gamma \phi_{j,i} \quad (2)$$

$$\varepsilon_{ij} = u_{j,i} + e_{jik} \phi_k \quad (3)$$

Where, t_{ij} is force stress tensor, m_{ij} is couple stress tensor, ε_{ij} is micro-strain tensor, ϕ_i is micro-rotation tensor, δ_{ij} is Kronecker delta and λ, μ^*, κ, α, β and γ are the six constants of micropolar elastic materials. κ, α *and* γ are the new micropolar constants which vanish for classical materials. The dimension of κ is force/length^2, and for α, β and γ it is forces (couple/length), and $i, j = x, y, z$. e_{jik} is the permutation symbol, and $u_{j,i} = \partial u_j / \partial x_j$, u_j is the displacement in j direction, x_i is the Cartesian coordinate in i direction. The limits for the micropolar constants are give by:

$$0 \leq 3\lambda + 2\mu^* + k \;,\; 0 \leq 2\mu^* + k \;,\; 0 \leq k \quad (4)$$

$$0 \leq 3\alpha + \beta + \gamma \;,\; -\gamma \leq \beta \leq \gamma \;,\; 0 \leq \gamma \quad (5)$$

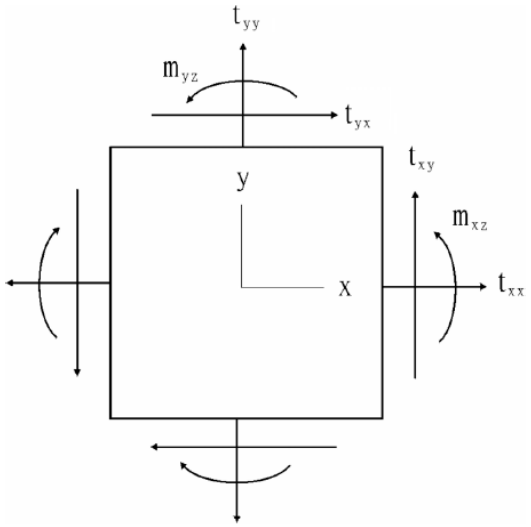

Fig. 1 Forces and Couple stress orientation for 2D case

Substituting (3) in (1) and (2) and arranging the resultant equation in terms of matrix form,

$$\begin{Bmatrix} t_{ij} \\ m_{ij} \end{Bmatrix} = [D_{ijkl}] \begin{Bmatrix} u \\ v \end{Bmatrix} \quad (6)$$

Where, $[D_{ijkl}]$ is the stiffness matrix. The forces and couple stress orientation for a two dimensional case is represented in Fig. 1, assuming that $\phi_x = \phi_z = 0$, the stress-strain relation [7] is given by:

$$\{\sigma\} = [D]\{\varepsilon\} \quad (7)$$

Where $[D]$ is the material property matrix, strain vector and stress vector for two dimensional problems are:

$$\{\varepsilon\} = \{\varepsilon_{xx}, \varepsilon_{yy}, \varepsilon_{xy}, \varepsilon_{yx}, \phi_{z,x} \phi_{z,y}\}^T = \left\{ \frac{\partial u}{\partial x}, \frac{\partial v}{\partial y}, \frac{\partial v}{\partial x} - \phi_z, \frac{\partial u}{\partial y} + \phi_z, \frac{\partial \phi_z}{\partial x}, \frac{\partial \phi_z}{\partial y} \right\}^T \quad (7a)$$

$$\{\sigma\} = \{t_{xx}, t_{yy}, t_{xy}, t_{yx}, m_{xz}, m_{yz}\}^T \quad (7b)$$

For the two dimensional Micropolar problem, to find the material property matrix there exists two cases: (a) Micropolar Plane Strain and (b) Micropolar Plane Stress conditions.

2.2 Micropolar Plane strain problem:

For the Micropolar plane strain condition, the only non-zero strains are $\varepsilon_{xx}, \varepsilon_{yy}, \varepsilon_{xy}, \varepsilon_{yx}, \phi_{z,x} \phi_{z,y}$ the rest of all strains are zeros. The corresponding material property matrix is:

$$[D] = \begin{bmatrix} \lambda+2\mu^*+k & \lambda & 0 & 0 & 0 & 0 \\ \lambda & \lambda+2\mu^*+k & 0 & 0 & 0 & 0 \\ 0 & 0 & \mu^*+k & \mu^* & 0 & 0 \\ 0 & 0 & \mu^* & \mu^*+k & 0 & 0 \\ 0 & 0 & 0 & 0 & \gamma & 0 \\ 0 & 0 & 0 & 0 & 0 & \gamma \end{bmatrix} \quad (8a)$$

2.3 Micropolar Plane stress problem:

For the Micropolar plane stress condition, the only non-zero stresses are $t_{xx}, t_{yy}, t_{xy}, t_{yx}, m_{xz}, m_{yz}$ and the rest of all stresses are zeros. The corresponding material property matrix is:

$$[D] = \begin{bmatrix} \frac{(2\mu^*+k)(2\lambda+2\mu^*+k)}{\lambda+2\mu^*+k} & \frac{\lambda(2\mu^*+k)}{\lambda+2\mu^*+k} & 0 & 0 & 0 & 0 \\ \frac{\lambda(2\mu^*+k)}{\lambda+2\mu^*+k} & \frac{(2\mu^*+k)(2\lambda+2\mu^*+k)}{\lambda+2\mu^*+k} & 0 & 0 & 0 & 0 \\ 0 & 0 & \mu^*+k & \mu^* & 0 & 0 \\ 0 & 0 & \mu^* & \mu^*+k & 0 & 0 \\ 0 & 0 & 0 & 0 & \gamma & 0 \\ 0 & 0 & 0 & 0 & 0 & \gamma \end{bmatrix} \quad (8b)$$

As mentioned earlier, λ, μ*, κ, α, β and γ are the six constants of Micropolar elastic materials and the relation between μ* and μ is given by the relation [8]: $\mu^* + \frac{k}{2} = \mu$, where λ and μ are the traditional Lamé's constants with the dimensions force/length^2.

As the values of α and β are zero in the case of 2D Micropolar theory, material property matrix *[D]* combines both force terms and couple stress in contrast to that of given by Namakura [9 - 10].

Gauthier gave the definitions of Micropolar Young's modulus and Micropolar Poisson's ratio [11], [12] as:

Micropolar Young's modulus, $$E_m = \frac{(2\mu^*+k)(3\lambda+2\mu^*+k)}{2\lambda+2\mu^*+k} \quad (9a)$$

Micropolar Poisson's ratio, $$\nu_m = \frac{\lambda}{2\lambda+2\mu^*+k} \quad (9b)$$

By taking the inverse of above two equations (9a) and (9b), we obtain:

Modulus of rigidity, $$G = \frac{E_m}{2(1+\nu_m)} = \frac{2\mu^*+k}{2} \quad (9c)$$

And $$\lambda = \frac{E_m \nu_m}{(1+\nu_m)(1-2\nu_m)} \quad (9d)$$

Namakura , defined a two constants, characteristic length and coupling factor as follows:

Characteristic length, $$l^2 = \frac{\gamma}{2(2\mu^*+k)} \quad (10a)$$

Coupling factor, $$N^2 = \frac{k}{2(\mu^*+k)} \quad (10b)$$

The value of *N* varies from 0 (i.e., Classical Elasticity Theory) to 1 (i.e., intermediate couple stresses theory) . The material property matrix for both plane strain and plane stress problem can be expressed in terms of this Micropolar Young's modulus, Micropolar Poisson's ratio, characteristic constant and coupling factor as:

Material matrix, *[D]* for plane strain problem is:

$$[D]=\begin{bmatrix} \frac{E_m(1-\nu_m)}{(1+\nu_m)(1-2\nu_m)} & \frac{E_m\nu_m}{(1+\nu_m)(1-2\nu_m)} & 0 & 0 & 0 & 0 \\ \frac{E_m\nu_m}{(1+\nu_m)(1-2\nu_m)} & \frac{E_m(1-\nu_m)}{(1+\nu_m)(1-2\nu_m)} & 0 & 0 & 0 & 0 \\ 0 & 0 & \frac{E_m}{2(1+\nu_m)(1-N^2)} & \frac{E_m(1-2N^2)}{2(1+\nu_m)(1-N^2)} & 0 & 0 \\ 0 & 0 & \frac{E_m(1-2N^2)}{2(1+\nu_m)(1-N^2)} & \frac{E_m}{2(1+\nu_m)(1-N^2)} & 0 & 0 \\ 0 & 0 & 0 & 0 & \frac{2E_m l^2}{(1+\nu_m)} & 0 \\ 0 & 0 & 0 & 0 & 0 & \frac{2E_m l^2}{(1+\nu_m)} \end{bmatrix} \quad (11a)$$

Material matrix, *[D]* for plane stress problem is:

$$[D]=\begin{bmatrix} \frac{E_m}{(1-\nu_m{}^2)} & \frac{E_m\nu_m}{(1-\nu_m{}^2)} & 0 & 0 & 0 & 0 \\ \frac{E_m\nu_m}{(1-\nu_m{}^2)} & \frac{E_m}{(1-\nu_m{}^2)} & 0 & 0 & 0 & 0 \\ 0 & 0 & \frac{E_m}{2(1+\nu_m)(1-N^2)} & \frac{E_m(1-2N^2)}{2(1+\nu_m)(1-N^2)} & 0 & 0 \\ 0 & 0 & \frac{E_m(1-2N^2)}{2(1+\nu_m)(1-N^2)} & \frac{E_m}{2(1+\nu_m)(1-N^2)} & 0 & 0 \\ 0 & 0 & 0 & 0 & \frac{2E_m l^2}{(1+\nu_m)} & 0 \\ 0 & 0 & 0 & 0 & 0 & \frac{2E_m l^2}{(1+\nu_m)} \end{bmatrix} \quad (11b)$$

2.3 Micropolar Plane stress problem:

For the Micropolar plane stress condition, the only non-zero stresses are $t_{xx}, t_{yy}, t_{xy}, t_{yx}, m_{xz}, m_{yz}$ and the rest of all stresses are zeros. The corresponding material property matrix is:

$$[D]=\begin{bmatrix} \frac{(2\mu^*+k)(2\lambda+2\mu^*+k)}{\lambda+2\mu^*+k} & \frac{\lambda(2\mu^*+k)}{\lambda+2\mu^*+k} & 0 & 0 & 0 & 0 \\ \frac{\lambda(2\mu^*+k)}{\lambda+2\mu^*+k} & \frac{(2\mu^*+k)(2\lambda+2\mu^*+k)}{\lambda+2\mu^*+k} & 0 & 0 & 0 & 0 \\ 0 & 0 & \mu^*+k & \mu^* & 0 & 0 \\ 0 & 0 & \mu^* & \mu^*+k & 0 & 0 \\ 0 & 0 & 0 & 0 & \gamma & 0 \\ 0 & 0 & 0 & 0 & 0 & \gamma \end{bmatrix} \quad (8b)$$

As mentioned earlier, λ, μ^*, κ, α, β and γ are the six constants of Micropolar elastic materials and the relation between μ^* and μ is given by the relation [8]: $\mu^* + \frac{k}{2} = \mu$, where λ and μ are the traditional Lamé's constants with the dimensions force/length^2.

As the values of α and β are zero in the case of 2D Micropolar theory, material property matrix *[D]* combines both force terms and couple stress in contrast to that of given by Namakura [9 - 10].

Gauthier gave the definitions of Micropolar Young's modulus and Micropolar Poisson's ratio [11], [12] as:

Micropolar Young's modulus, $E_m = \dfrac{(2\mu^* + k)(3\lambda + 2\mu^* + k)}{2\lambda + 2\mu^* + k}$ (9a)

Micropolar Poisson's ratio, $\nu_m = \dfrac{\lambda}{2\lambda + 2\mu^* + k}$ (9b)

By taking the inverse of above two equations (9a) and (9b), we obtain:

Modulus of rigidity, $G = \dfrac{E_m}{2(1+\nu_m)} = \dfrac{2\mu^* + k}{2}$ (9c)

And $\lambda = \dfrac{E_m \nu_m}{(1+\nu_m)(1-2\nu_m)}$ (9d)

Namakura , defined a two constants, characteristic length and coupling factor as follows:

Characteristic length, $l^2 = \dfrac{\gamma}{2(2\mu^* + k)}$ (10a)

Coupling factor, $N^2 = \dfrac{k}{2(\mu^* + k)}$ (10b)

The value of *N* varies from 0 (i.e., Classical Elasticity Theory) to 1 (i.e., intermediate couple stresses theory) . The material property matrix for both plane strain and plane stress problem can be expressed in terms of this Micropolar Young's modulus, Micropolar Poisson's ratio, characteristic constant and coupling factor as:

Material matrix, *[D]* for plane strain problem is:

$$[D] = \begin{bmatrix} \frac{E_m(1-\nu_m)}{(1+\nu_m)(1-2\nu_m)} & \frac{E_m\nu_m}{(1+\nu_m)(1-2\nu_m)} & 0 & 0 & 0 & 0 \\ \frac{E_m\nu_m}{(1+\nu_m)(1-2\nu_m)} & \frac{E_m(1-\nu_m)}{(1+\nu_m)(1-2\nu_m)} & 0 & 0 & 0 & 0 \\ 0 & 0 & \frac{E_m}{2(1+\nu_m)(1-N^2)} & \frac{E_m(1-2N^2)}{2(1+\nu_m)(1-N^2)} & 0 & 0 \\ 0 & 0 & \frac{E_m(1-2N^2)}{2(1+\nu_m)(1-N^2)} & \frac{E_m}{2(1+\nu_m)(1-N^2)} & 0 & 0 \\ 0 & 0 & 0 & 0 & \frac{2E_m l^2}{(1+\nu_m)} & 0 \\ 0 & 0 & 0 & 0 & 0 & \frac{2E_m l^2}{(1+\nu_m)} \end{bmatrix}$$

(11a)

Material matrix, *[D]* for plane stress problem is:

$$[D]=\begin{bmatrix} \frac{E_m}{(1-\nu_m{}^2)} & \frac{E_m\nu_m}{(1-\nu_m{}^2)} & 0 & 0 & 0 & 0 \\ \frac{E_m\nu_m}{(1-\nu_m{}^2)} & \frac{E_m}{(1-\nu_m{}^2)} & 0 & 0 & 0 & 0 \\ 0 & 0 & \frac{E_m}{2(1+\nu_m)(1-N^2)} & \frac{E_m(1-2N^2)}{2(1+\nu_m)(1-N^2)} & 0 & 0 \\ 0 & 0 & \frac{E_m(1-2N^2)}{2(1+\nu_m)(1-N^2)} & \frac{E_m}{2(1+\nu_m)(1-N^2)} & 0 & 0 \\ 0 & 0 & 0 & 0 & \frac{2E_m l^2}{(1+\nu_m)} & 0 \\ 0 & 0 & 0 & 0 & 0 & \frac{2E_m l^2}{(1+\nu_m)} \end{bmatrix} \quad (11b)$$

3. Finite Element Formulation:

3.1 Linear Triangular Element:

A linear triangular element with three degrees of freedom at each node is considered as shown in Fig. 2. For a linear triangular element, shape functions are linear over the element [13].

The displacements u, v and ϕ_z are expressed in terms of shape functions and nodal values of unknown displacements as:

$$\{u\}=[N]\{q\} \quad (12)$$

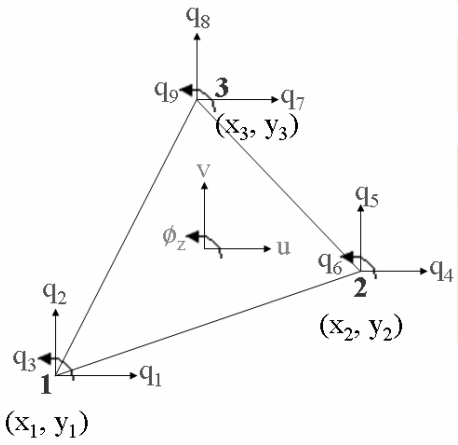

Fig. 2 Linear Triangular Element

The relation among the three shape functions is given by:

$$N_1+N_2+N_3=1 \quad (13)$$

$$N_1=\xi, N_2=\eta, N_3=\zeta=1-\xi-\eta \quad (14)$$

Where ξ, η and ζ are the natural coordinates. Where, $\{u\}=\{u,v,\phi_z\}^T$, displacement vector, *[N]* is shape function matrix and $\{q\}=\{q_1,q_2,q_3,q_4,q_5,q_6,q_7,q_8,q_9\}^T$, element displacement vectors. The shape function matrix *[N]* is given by [14]:

$$[N]=\begin{bmatrix} N_1 & 0 & 0 & N_2 & 0 & 0 & N_3 & 0 & 0 \\ 0 & N_1 & 0 & 0 & N_2 & 0 & 0 & N_3 & 0 \\ 0 & 0 & N_1 & 0 & 0 & N_2 & 0 & 0 & N_3 \end{bmatrix} \quad (15)$$

Using the chain rule, the relation between strain, displacement and micro-rotation vector is given by

$$\{\varepsilon\}=[B]\{q\} \quad (16)$$

$$\{\sigma\}=[D]\{\varepsilon\}=[D][B]\{q\} \quad (17)$$

$$[B]=\frac{1}{\det J}\begin{bmatrix} y_{23} & 0 & 0 & y_{31} & 0 & 0 & y_{12} & 0 & 0 \\ 0 & x_{32} & 0 & 0 & x_{13} & 0 & 0 & x_{21} & 0 \\ 0 & y_{23} & -(\det J)\xi & 0 & y_{31} & -(\det J)\eta & 0 & y_{12} & -(\det J)\zeta \\ x_{32} & 0 & (\det J)\xi & x_{13} & 0 & (\det J)\eta & x_{21} & 0 & (\det J)\zeta \\ 0 & 0 & y_{23} & 0 & 0 & y_{31} & 0 & 0 & y_{12} \\ 0 & 0 & x_{32} & 0 & 0 & x_{13} & 0 & 0 & x_{21} \end{bmatrix} \quad (18)$$

The matrix *[B]* is known as element strain-displacement matrix.

3.2 Energy method:

Using the principle of total potential energy, the total potential energy can be written as

$$\prod = U + V \quad (19)$$

Considering, applied body force and body couple (G_i, C_i) and applied surface force, surface traction (T_i, M_i), [7] and if u_i and ϕ_i are displacement and micro-rotation along i – direction, the total potential energy can be written as:

$$\prod = \frac{1}{2}\iiint_v \{t_{ji}\varepsilon_{ji} + m_{ji}\phi_{ij}\}dv - \iiint_v \{G_i u_i + C_i\phi_i\}dv - \int_s \{T_i^{(u)} + M_i^{(v)}\phi_i\}ds \quad (20)$$

Using equations (12) to (18) the total energy becomes:

$$\prod_e = \frac{1}{2}\{q^e\}^T[K^e]\{q^e\} - \{q^e\}^T\left(\{F_v^e\} + \{F_s^e\}\right) \quad (21)$$

Where, element stiffness matrix, $[K^e] = \iiint_v \left([B]^T[D][B]\right)dv$ (22)

Element body force and body couple, $\{F_v^e\} = \iiint_v \left([N]^T\{\{G\} + \{C\}\}\right)dv$ (23)

Element surface force and surface traction, $\{F_s^e\} = \int_s \left([N]^T\{\{T^{(v)}\} + \{M^{(v)}\}\}\right)ds$ (24)

The total structural potential energy is the summation of total element strain energy:

$$\prod = \sum \prod_e \quad (25)$$

Substituting (21) into (25) and now using the principle of minimum potential energy,

$$\frac{\partial \prod}{\partial\{q\}} = 0 \quad (26)$$

The resultant equation will become:

$$[K]\{q\} = \{F_v\} + \{F_s\} \tag{27}$$

3.3 Numerical Integration:

For getting stiffness matrix, integral is to be solved which can be done by using numerical integration technique. Gaussian quadrature integration technique with triangular sampling points is used for solving this integral. Assuming that depth *t* of the triangular element is invariant,

$$dV = dx.dy.dz = t.dx.dz = t.\det J.d\xi.d\eta = t.2A.d\xi.d\eta \tag{28}$$

Where, *A* is the area of the linear triangular element. Applying this numerical integration technique for finding the stiffness matrix, i.e., equation (22) then,

$$[K^e] = \iiint_{V_e} \left([B]^T[D][B]\right)dV = \iint \left([B]^T[D][B]\right)2A.t.d\xi.d\eta$$

$$= 2A.t.\int_0^1 \int_0^{1-\xi} \left([B]^T[D][B]\right)d\xi.d\eta$$

$$= 2A.t.\int_0^1 \int_0^{1-\xi} f(\xi,\eta,\zeta)d\xi.d\eta$$

$$= 2A.t.\sum_{i=1}^{n} W_i f(\xi_i,\eta_i,\zeta_i) \tag{29}$$

3.3 Modal Analysis:

In this work, modal analysis was done for the various nylon plates considering it as a multi degree of freedom system; because the system will have a total of 10 degrees of freedom for Classical Elasticity Theory and 15 degrees of freedom for Micropolar Elasticity Theory.

Considering an un-damped free vibration case, the equation of motion was given by [15]:

$$[M]\{\ddot{q}\} + [K]\{q\} = \{0\} \tag{30}$$

The characteristic equation of Eigen value problem for an un-damped free vibration is given by:

$$\left([K] - \omega^2[M]\right)\{q\} = 0 \tag{31}$$

The term, $\left([K] - \omega^2[M]\right)$ is known as dynamic stiffness matrix, *{q}* contains only those DOF that assumes nonzero values after all rigid body modes and mechanisms are suppressed. Lumped mass matrix assumption was made for the ease of computations. The 'n' natural frequencies ω_r (r=1, 2…n) are obtained from above equation. The vector $\{q_r\}$, known as characteristic vectors or Eigen vectors and were normalized so that they will satisfy the ortho-normality conditions:

$$\{q\}^T[M]\{q\} = 1, r = 1,2...n$$
$$\{q\}^T[K]\{q\} = \omega^2, r = 1,2...n \quad \text{and} \tag{33}$$

4. ANSYS Model:

ANSYS model of the rectangular plate was created and meshing was done using (free mesh using triangular elements) PLANE42 element. The boundary conditions were assumed to be same as that was assumed in the code. The meshed model with boundary conditions using ANSYS was shown in Fig. 3(a). The plane strain and plane stress assumptions were simultaneously made for analysis of corresponding strains and structural Poisson's ratio.

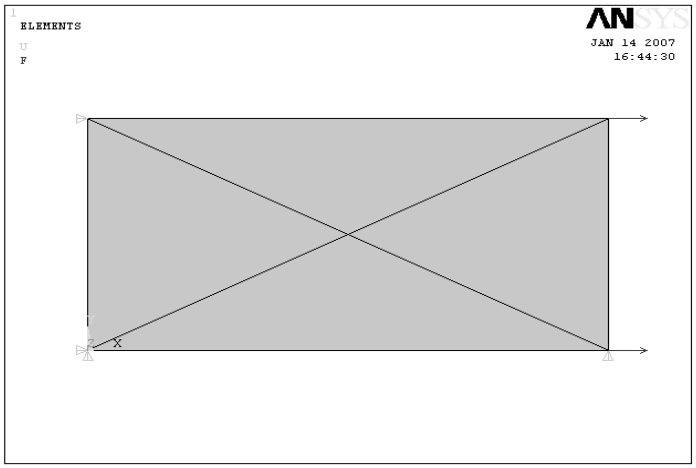

Fig. 3(a) Meshed ANSYS model of rectangular plate

5. Summary of Applications of various nylon materials used:

The following tables, gives properties and applications of various nylon materials chosen both glass filled and carbon filled for analysis purpose in this work and the material numbers given in Table 1 and 2 were used for further reference.

Table No. 1 Properties and Applications of GF Nylon Materials

GF Mat No.	Commercial Name	Tensile Modulus (MPa)	Mass Density (gm/cc)	Applications
1	PA 140/1 GF 33, 33% Glass Fiber, DAM[16]	10.48×10^3	1.41	Automotive Housings, Power Tool Housings
2	PA 140/1 GF 33, 33% Glass Fiber, Conditioned [17]	8.48×10^3	1.41	Bearings, Gears, Connectors,Automotive Housings, Power Tool, Housings
3	N6-G33L 33% GFR Nylon 6 [17]	13×10^3	1.46	Bearings, Gears, Automotive wheel covers, plated, High tolerance electrical switch boxes and connectors
4	Zytel (72G33L) [19]	5860	1.38	housings
5	Zytekl(82G33L) [19]	4480	1.34	Appliance-housings, hoses, jackets,tubes
6	PA 140/1 GF 30 [19]	7250	1.36	
7	PA 140/1 GF 33 [19]	8480	1.41	Gears, cams,auto, Indust
8	Ultramid A3EG6 [19]	7380	1.35	Housings, Insulators
9	DSM J-1/33HS [19]	8270	1.39	Insulators
10	Fiberfil TN J-8/33/IT [19]	6890	1.38	Appliances, automotive
11	RTP 205.3 [19]	1.17×10^4	1.39	Housings, automotive (exterior)
12	RTP 205.3 HS SI [19]	1.10×10^4	1.4	-
13	Thermofil N3-33FG-0103 [19]	1.03×10^4	1.4	General purpose
14	Thermofil N3-33FG-0214 [19]	9170	1.48	General purpose
15	Thermofil N3-33FG-0700 [19]	8960	1.38	Casters, handles
16	Thermofil N3-33FG-0727 [19]	7580	1.38	Pulleys, wheels, auto and machine parts
17	Thermofil N3-33FG-1100 [19]	1×10^4	1.4	Profile, rod and tube
18	Unfilled [18]	350×10^3	-	-

Table No. 2 Properties and Applications of CF Nylon Materials

CF Mat No.	Commercial Name	Tensile Modulus (MPa)	Mass Density (gm/cc)	Applications
1	DSM G-1/CF/30 [19]	2.41x 10^4	1.28	General purpose
2	Electrafil CF/30/TF13s12 [19]	2.78x 10^4	1.32	Automotive and electrical
3	Electrafil J-1/CF/30 [19]	2.07x 10^4	1.28	Electronic
4	Nybex 23000 BKV CF30 [19]	2.28x 10^4	1.33	Friction
5	RTP 285H CF30 [19]	2.14x 10^4	1.28	Electronic
6	RTP 285P CF30 [19]	1.72x 10^4	1.22	-
7	RTP 287P CF30 [19]	1.93x 10^4	1.28	-
8	RTP 299X51265F [19]	5170	1.35	Thermal
9	RTP 205.3 HS SI [19]	1.10x 10^4	2.15	-

6. Results and Discussion:

A simple rectangular element, meshed with four linear triangular elements as shown in Fig. 3(b), was used for analysis using code. The rectangular plate is assumed to be 10 mm long, 5 mm width and 1 mm thick. The loading conditions for the rectangular plate are $\tau_{xx} = 4MPa$ and $\tau_{yy} = \tau_{xy} = \tau_{yx} = m_{xy} = 0$. The boundary nodal forces F, applied are shown in Fig. 3(b).

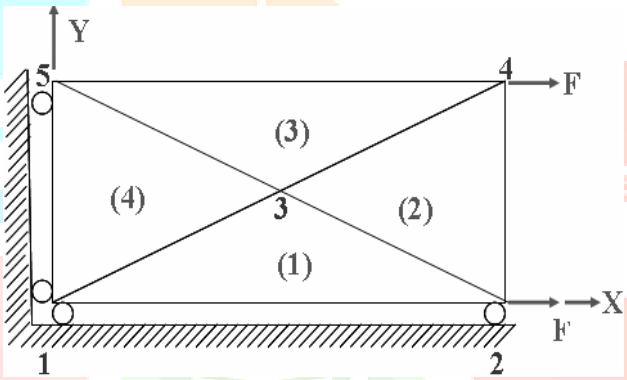

Fig. 3(b) 2-Elements, 4-noded rectangular plate

The Micropolar constants chosen for the analysis are: λ = 2 x 10^6 MPa, μ* = 2 x 10^6 MPa, κ= 0, γ = 8 x 10^8 MPa, α = β = 0. Micropolar Poisson's ration, ν_m = 0.25, Modulus of Rigidity. The characteristic length, l =10 mm and coupling factor, N =0.0 [8].

(a) Results for glass filled nylon plate:

The average longitudinal and lateral strains and structural Poisson's ratio for glass filled nylon plate was shown in Table No. 3. It is depicted that the Structural Poisson's ratio of the deformed rectangular plate after application of the load remains same for all glass filled nylon materials even though there is variation in strains of different materials, i.e., 0.333333 for the plane strain condition and 0.250 for the case of plane stress condition. The variations of strains ε_{xx} and ε_{yy} for different materials using Micropolar Elasticity Theory and Classical Theory of Elasticity were shown in Fig.4 and Fig. 5; also the corresponding Poisson's ratios are shown in Fig.6.

Table 3 Strains and Poisson's ratios for different glass filled nylon materials

GF Mat No.	Plane Strain Condition			Plane Stress Condition		
	Avg. ε_{xx}	Avg. ε_{yy}	Structural ν	Avg. ε_{xx}	Avg. ε_{yy}	Structural ν
01	2.73E-4	-9.09E-5	0.333333333	2.86E-4	-7.16E-5	0.25
02	3.37E-4	-1.12E-4	0.333333333	3.54E-4	-8.84E-5	0.25
03	2.20E-4	-7.33E-5	0.333333333	2.31E-4	-5.77E-5	0.25
04	4.88E-4	-1.63E-4	0.333333333	5.12E-4	-1.28E-4	0.25
05	7.25E-4	-2.02E-4	0.333333333	6.90E-4	-1.91E-4	0.25
06	3.94E-4	-1.31E-4	0.333333333	4.14E-4	-1.03E-4	0.249999
07	3.37E-4	-1.12E-4	0.333333333	3.54E-4	-8.84E-5	0.25
08	4.56E-4	-1.25E-4	0.333333333	4.52E-4	-1.08E-4	0.25
09	3.45E-4	-1.15E-4	0.333333333	3.63E-4	-9.07E-5	0.25
10	4.15E-4	-1.8E-4	0.333333333	4.35E-4	-1.09E-4	0.25
11	2.44E-4	-8.14E-5	0.333333333	2.56E-4	-6.41E-5	0.24999
12	2.60E-4	-8.66E-5	0.333333333	2.73E-4	-6.82E-5	0.25
13	2.77E-4	-9.25E-5	0.333333333	2.91E-4	-7.28E-5	0.25
14	3.12E-4	-1.04E-4	0.333333333	3.27E-4	-8.18E-5	0.25
15	3.65E-4	-1.04E-4	0.333333333	3.68E-4	-8.20E-5	0.25
16	3.77E-4	-1.26E-4	0.333333333	3.96E-4	-9.89E-5	0.249
17	2.07E-4	-6.90E-5	0.333333333	3.64E-4	-5.40E-5	0.25
18	8.16E-6	-2.72E-6	0.333333333	8.57E-6	-2.14E-6	0.25

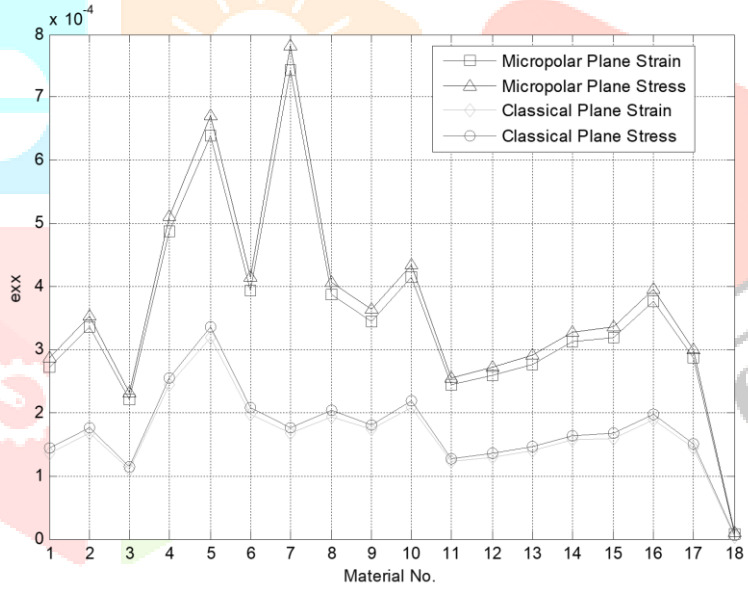

Fig. 4 Variation of Micropolar and Classical ε_{xx} for different nylon GF materials

From the Fig.4, if we exclude the unfilled material, it was clear that for N6-G33L 33% GFR Nylon 6, i.e., for material no. 03, the longitudinal strains (ε_{xx}) is minimum and the same is maximum for Zytel (82G33L) (GF Mat No. 05) for both plane strain and plane stress conditions. If unfilled material is also considered, ε_{xx} is minimum for Noryl Unfilled (GF Mat No. 18).

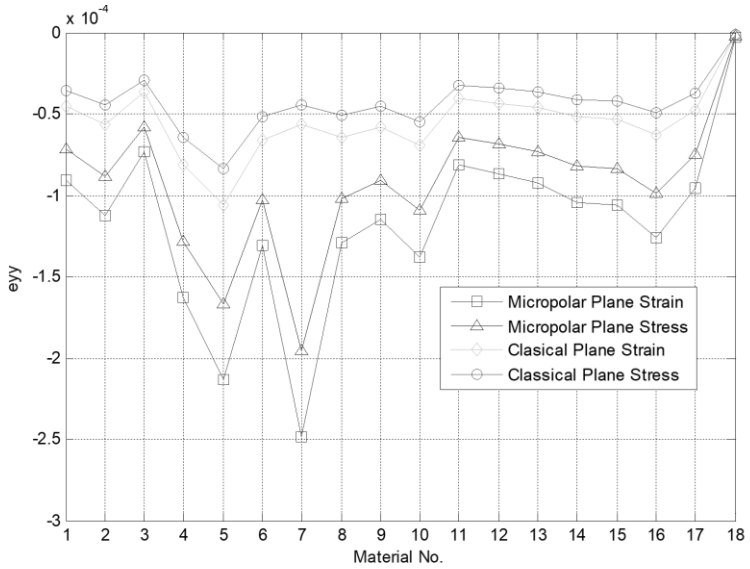

Fig. 5 Variation of Micropolar and Classical ε_{yy} for different nylon GF materials

From Fig. 5, Lateral strain, ε_{yy} is minimum for Zytel(82G33L) (GF Mat No. 05) and maximum for N6-G33L 33% GFR Nylon 6 (GF Mat No. 03) for both plane strain and plane stress conditions If unfilled material is also considered, εyy is maximum for Noryl Unfilled (GF Mat No. 18). The structural Poisson's ratio remains constant for both the theories and for plane strain and plane stress respectively, was shown in Fig. 6.

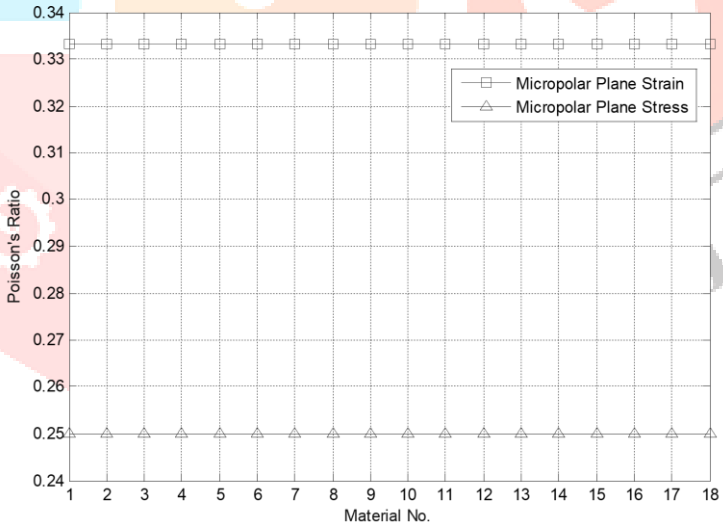

Fig. 6 Micropolar Poisson's ratio for different types of glass filled nylon GF materials

(b) Results for Carbon filled nylon plate:

Table No. 4 gives the average longitudinal, lateral strains and structural Poisson's ratio for carbon filled nylon plate.

Table 4 Strains and Poisson's ratio for different carbon filled nylon materials

CF Mat No.	Plane Strain Condition			Plane Stress Condition		
	Avg. ε_{xx}	Avg. ε_{yy}	Structural ν	Avg. ε_{xx}	Avg. ε_{yy}	Structural ν
01	1.19E-04	-3.95E-05	0.33333333	1.24E-04	-3.11E-05	0.25
02	1.03E-04	-3.43E-05	0.33333333	1.08E-04	-2.70E-05	0.25
03	1.29E-05	-4.26E-05	0.33333333	1.34E-04	-3.55E-05	0.25
04	1.25E-04	-4.18E-05	0.33333333	1.32E-04	-3.29E-05	0.25
05	1.34E-04	-4.45E-05	0.33333333	1.40E-04	-3.50E-05	0.25
06	1.66E-04	-5.54E-05	0.33333333	1.74E-04	-4.36E-05	0.25
07	1.48E-04	-4.93E-05	0.33333333	1.55E-04	-3.89E-05	0.25
08	2.60E-04	-8.66E-05	0.33333333	2.73E-04	-6.82E-05	0.25
09	5.53E-04	-1.84E-04	0.33333333	5.80E-04	-1.45E-04	0.25

From Fig. 7, it is depicted, ε_{xx} is minimum for Electrafil-CF/30/TF13s12 (GF Mat No.02) and maximum for RTP 299X51265F (GF Mat No. 09) for both plane strain and plane stress conditions. εyy is minimum for RTP 299X51265F (GF Mat No.09) and maximum for Electrafil CF/30/TF13s12 (GF Mat No. 02) for both plane strain and plane stress conditions.

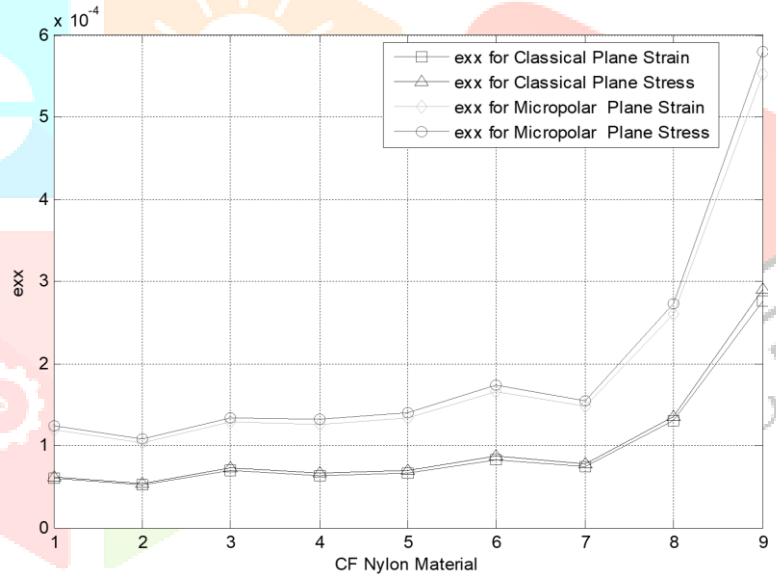

Fig. 7 Variation of Micropolar and Classical ε_{xx} for different nylon CF materials

From Fig. 7, the longitudinal strain (ε_{xx}) is minimum for Electrafil CF/30/TF13s12 (CF Mat No 2) and maximum for RTP 299X51265F (CF Mat No .8). From Fig. 8, the lateral strain (ε_{yy}) is minimum for RTP 299X51265F (GF Mat No.09) and maximum for Electrafil CF/30/TF13s12 (GF Mat No. 02) for both plane strain and plane stress conditions.

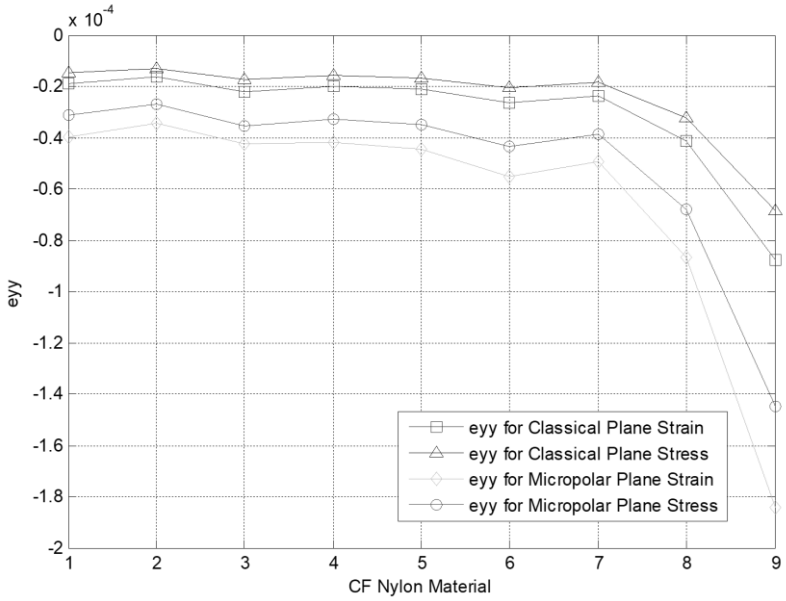

Fig. 8 Variation of Micropolar and Classical ε_{yy} for different nylon CF materials

From Fig 9, similar to the case of glass filled nylon materials, also for carbon filled nylon materials, there is no change in the structural Poisson's ratio but there exists corresponding change in their strains.

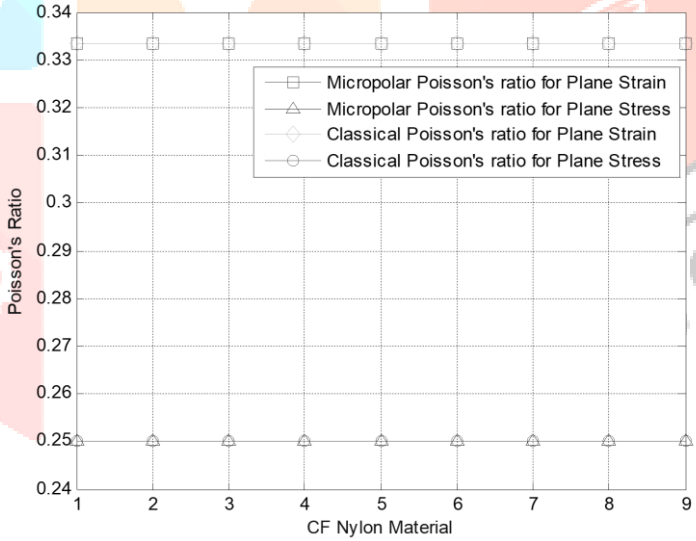

Fig. 9 Poisson's Ratio for different types of nylon carbon filled materials

(c) Validation of program results:

The strains obtained for various nylon materials using classical elasticity theory by program were validated with those of ANSYS results.

The comparison of longitudinal strains and lateral strains between program results and those obtained from ANSYS software for glass filled nylon materials were given in Fig. 10 and Fig. 11 respectively, and the error percentage was found to be 0.0619 and 0.0618 respectively.

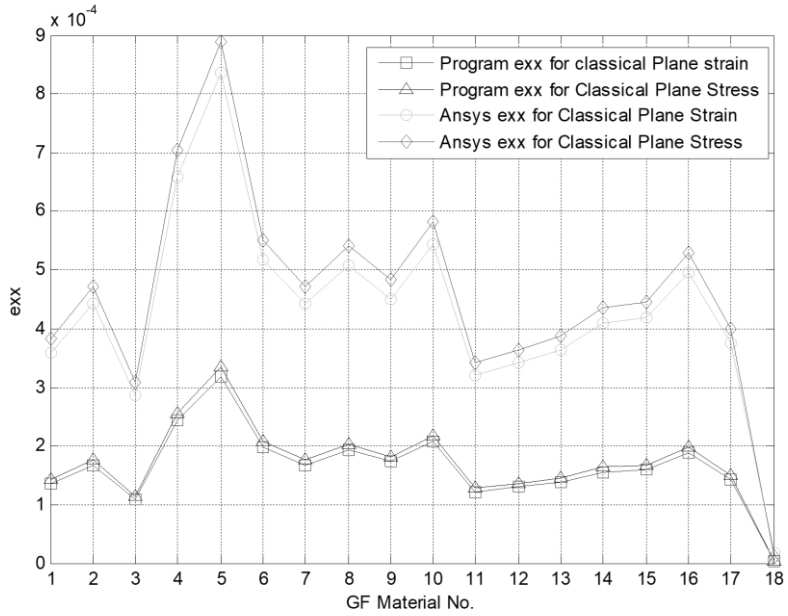

Fig. 10 Comparison of Program ε_{xx} and ANSYS ε_{xx} for CET for GF Nylon Material

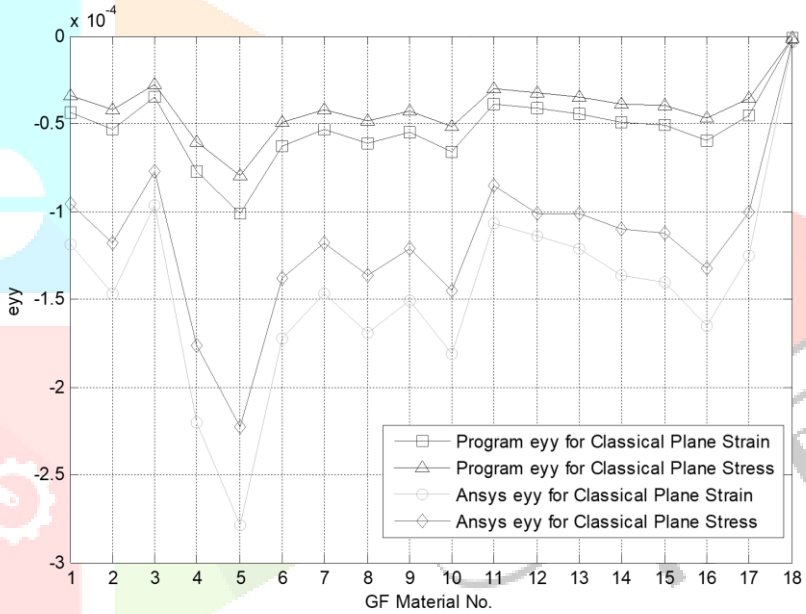

Fig. 11 Comparison of Program ε_{yy} and ANSYS ε_{yy} for CET for GF Nylon Material

The comparison of longitudinal strains and lateral strains for carbon filled nylon materials between program results and those obtained from ANSYS software were given in Fig. 12 and Fig. 13 respectively, and the error percentage was found to be 0.0619 for both the cases.

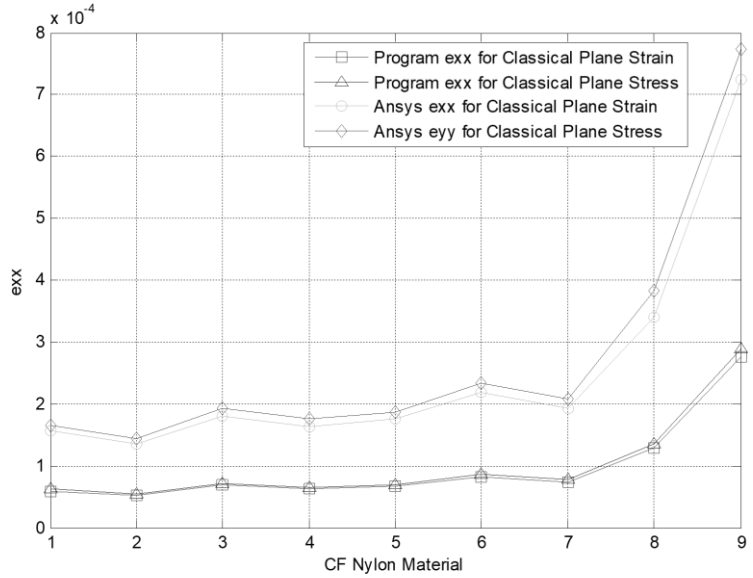

Fig. 12 Comparison of Program ε_{xx} and ANSYS ε_{xx} for CET for CF Nylon Material

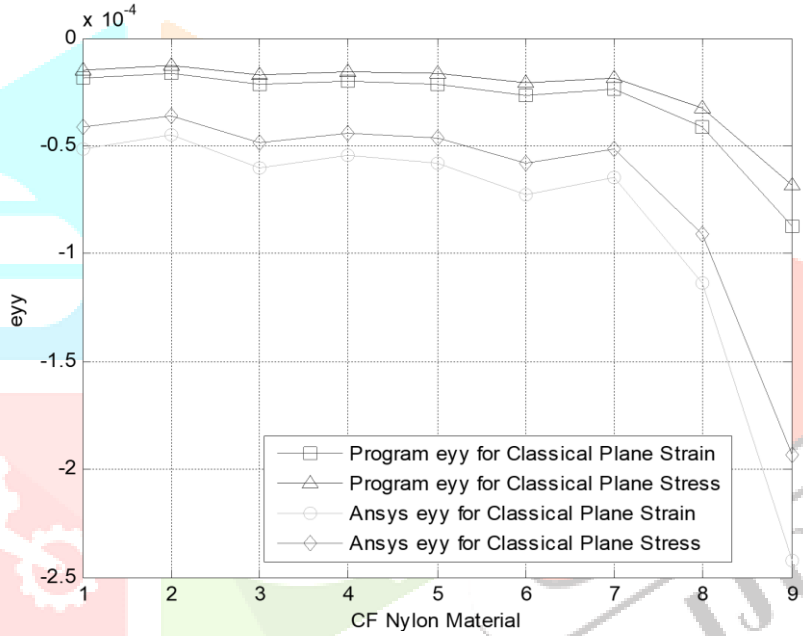

Fig. 13 Comparison of Program ε_{xx} and ANSYS ε_{xx} for CET for CF Nylon Material

7. Results of Modal Analysis:

(a) Using Classical Theory of Elasticity:

The modal analysis (un-damped free vibration) was done for various nylon plates considering the plane strain assumption using both Classical Elasticity Theory and Micropolar Elasticity theory. For the case of CET, the system will have a total of 10 DOF among them, 4 DOF were fixed so that, the natural frequencies corresponding to these DOF were zero or very near to zero. Thus, the other natural frequencies (corresponding to other 6 DOF and 4 fixed DOF) obtained using the CET was given in Table 5.

Table 5 Natural Frequencies of different glass filled nylon plate using CET

GF Mat No.	Eigen Values									
	1	2	3	4	5	6	7	8	9	10
1	0	0	0	5.22 E-11	5.96 E+4	1.12 E+5	1.14 E+5	1.27 E+5	1.83 E+5	2.53 E+5
2	4.83 E-11	0	0	0	5.36 E+4	1.01 E+5	1.02 E+5	1.14 E+5	1.64 E+5	2.28 E+5
3	7.28 E-11	0	0	0	6.52 E+4	1.23 E+5	1.24 E+5	1.39 E+5	2.00 E+5	2.77 E+5
4	0	0	0	1.63 E-11	1.42 E+4	2.68 E+4	2.72 E+4	3.04 E+4	4.36 E+4	6.06 E+4
5	1.01 E-11	0	0	0	1.26 E+4	2.38 E+4	2.41 E+4	2.69 E+4	3.87 E+4	5.37 E+4
6	0	0	0	2.66 E-11	1.60 E+4	3.00 E+4	3.04 E+4	3.40 E+4	4.89 E+4	6.79 E+4
7	1.91 E-11	0	0	0	1.70 E+4	3.19 E+4	3.23 E+4	3.61 E+4	5.19 E+4	7.21 E+4
8	1.77 E-11	0	0	0	1.62 E+4	3.04 E+4	3.08 E+4	3.45 E+4	4.95 E+4	6.87 E+4
9	0	0	2.86 E-25	1.78 E-11	1.69 E+4	3.17 E+4	3.22 E+4	3.60 E+4	5.16 E+4	7.17 E+4
10	0	0	0	1.83 E-11	1.54 E+4	2.90 E+4	2.95 E+4	3.29 E+4	4.73 E+4	6.57 E+4
11	0	0	0	1.46 E-11	2.01 E+4	3.77 E+4	3.82 E+4	4.28 E+4	6.14 E+4	8.53 E+4
12	1.74 E-11	0	0	0	1.94 E+4	3.64 E+4	3.69 E+4	4.13 E+4	5.94 E+4	8.24 E+4
13	0	0	0	2.61 E-11	1.88 E+4	3.52 E+4	3.58 E+4	4.00 E+4	5.74 E+4	7.97 E+4
14	1.47 E-11	0	0	0	1.72 E+4	3.23 E+4	3.28 E+4	3.67 E+4	5.27 E+4	7.32 E+4
15	1.04 E-11	0	0	0	1.76 E+4	3.31 E+4	3.36 E+4	3.76 E+4	5.40 E+4	7.49 E+4
16	0	0	0	1.97 E-11	1.62 E+4	3.04 E+4	3.09 E+4	3.45 E+4	4.96 E+4	6.89 E+4
17	1.47 E-11	0	0	0	1.85 E+4	3.47 E+4	3.52 E+4	3.94 E+4	5.66 E+4	7.86 E+4

The Fig. 14, shows the natural frequencies for different glass filled nylon materials obtained using CET. Natural frequency

(ω_{10}) is maximum for N6-G33L 33% GFR+ (GF Mat No. 03) ω_{10} is minimum for Zytel (82G33L) (GF Mat No. 05), as the first four natural frequencies corresponds to those DOF which are fixed at nodes, they have zero value of natural frequency

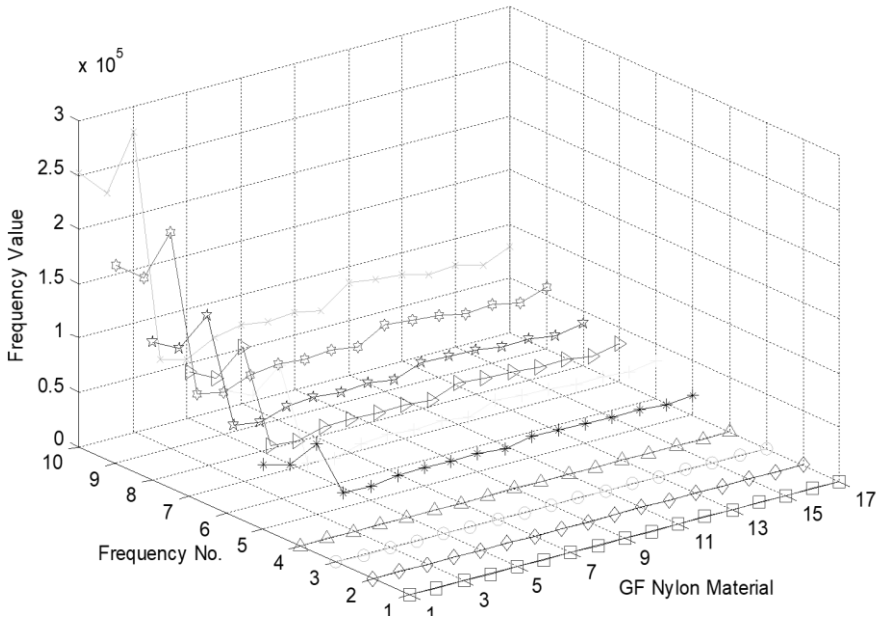

Fig. 14 Natural Frequency using Classical Elasticity Theory for GF Nylon Materials

The natural frequencies of carbon filled nylon plate using CET were given in Table No. 6 and the same were plotted in Fig. 15. The natural frequency (ω_{10}) is maximum for Electrafil CF/30/TF13s12 (GF Mat No. 02) ω_{10} is minimum for RTP 299X51265F (GF Mat No. 08).

Table 6 Natural Frequencies of different carbon filled nylon plate using CET

GF Mat No.	Eigen Values									
	1	2	3	4	5	6	7	8	9	10
1	0	0	0	5.22 E-11	5.96 E+4	1.12 E+5	1.14 E+5	1.27 E+5	1.83 E+5	2.53 E+5
2	4.83 E-11	0	0	0	5.36 E+4	1.01 E+5	1.02 E+5	1.14 E+5	1.64 E+5	2.28 E+5
3	7.28 E-11	0	0	0	6.52 E+4	1.23 E+5	1.24 E+5	1.39 E+5	2.00 E+5	2.77 E+5
4	0	0	0	1.63 E-11	1.42 E+4	2.68 E+4	2.72 E+4	3.04 E+4	4.36 E+4	6.06 E+4
5	1.01 E-11	0	0	0	1.26 E+4	2.38 E+4	2.41 E+4	2.69 E+4	3.87 E+4	5.37 E+4
6	0	0	0	2.66 E-11	1.60 E+4	3.00 E+4	3.04 E+4	3.40 E+4	4.89 E+4	6.79 E+4
7	1.91 E-11	0	0	0	1.70 E+4	3.19 E+4	3.23 E+4	3.61 E+4	5.19 E+4	7.21 E+4
8	1.77 E-11	0	0	0	1.62 E+4	3.04 E+4	3.08 E+4	3.45 E+4	4.95 E+4	6.87 E+4
9	0	0	2.86 E-25	1.78 E-11	1.69 E+4	3.17 E+4	3.22 E+4	3.60 E+4	5.16 E+4	7.17 E+4
10	0	0	0	1.83 E-11	1.54 E+4	2.90 E+4	2.95 E+4	3.29 E+4	4.73 E+4	6.57 E+4
11	0	0	0	1.46 E-11	2.01 E+4	3.77 E+4	3.82 E+4	4.28 E+4	6.14 E+4	8.53 E+4
12	1.74 E-11	0	0	0	1.94 E+4	3.64 E+4	3.69 E+4	4.13 E+4	5.94 E+4	8.24 E+4
13	0	0	0	2.61 E-11	1.88 E+4	3.52 E+4	3.58 E+4	4.00 E+4	5.74 E+4	7.97 E+4
14	1.47 E-11	0	0	0	1.72 E+4	3.23 E+4	3.28 E+4	3.67 E+4	5.27 E+4	7.32 E+4
15	1.04 E-11	0	0	0	1.76 E+4	3.31 E+4	3.36 E+4	3.76 E+4	5.40 E+4	7.49 E+4
16	0	0	0	1.97 E-11	1.62 E+4	3.04 E+4	3.09 E+4	3.45 E+4	4.96 E+4	6.89 E+4

17	1.47 E-11	0	0	0	1.85 E+4	3.47 E+4	3.52 E+4	3.94 E+4	5.66 E+4	7.86 E+4

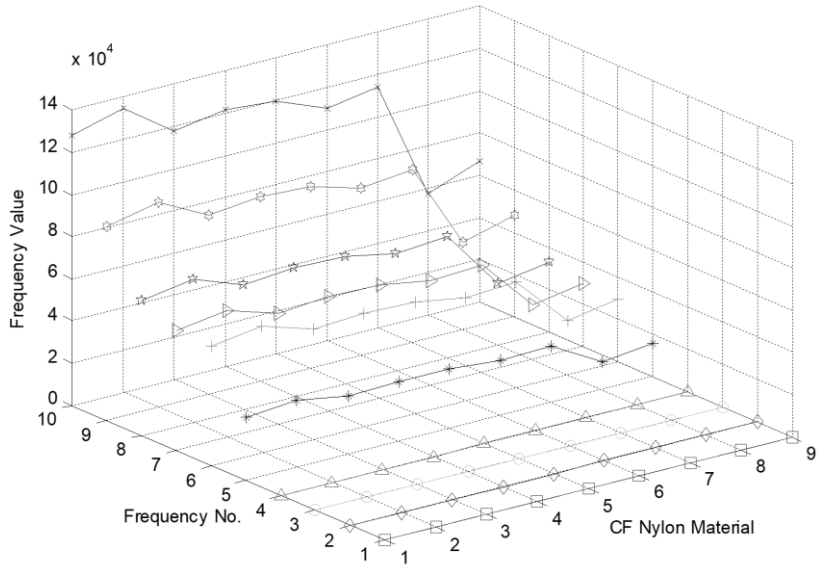

Fig. 15 Frequency Plot using Micropolar Theory for GF Nylon Materials

(b) Using Micropolar Elasticity Theory:

Modal analysis was also done using Micropolar Elasticity Theory. As previously mentioned, considering MET causes the addition of one more DOF (rotation about z-axis) at all the nodes, then the system have totally 15 DOF, of those, 4 DOF were fixed as a result the no. of non-zero natural frequencies are 11. Here it is to be noted that the natural frequency corresponding rotational DOF at node 1 will have a very less value but not zero. Table 7 gives the natural frequencies of different glass filled nylon materials.

Table 7 Natural frequencies of different glass filled nylon plate using MET

GF Mat No.	Natural Frequency (ω_n)														
	1	2	3	4	5	6	7	8	9	10	11	12	13	14	15
1	2.7 E-1	0	0	0	1.2 E-3	1.62 E+4	2.43 E+4	3.21 E+4	3.58 E+4	5.15 E+4	6.99 E+4	3.27 E+5	5.17 E+5	6.54 E+5	8.96 E+5
2	2.5 E-5	1.6 E-8	0	0	1.7 E-3	1.46 E+4	2.18 E+4	2.89 E+4	3.22 E+4	4.64 E+4	6.29 E+4	2.94 E+5	4.65 E+5	5.89 E+5	8.06 E+5
3	8.7 E-4	1.67E-12	0	0	3.2 E-3	1.78 E+4	2.66 E+4	3.51 E+4	3.92 E+4	5.64 E+4	7.65 E+4	3.58 E+5	5.66 E+5	7.16 E+5	9.81 E+5
4	6.6 E-4	0	0	0	2.6 E-3	1.23 E+4	1.83 E+4	2.43 E+4	2.70 E+4	3.90 E+4	5.28 E+4	2.47 E+5	3.91 E+5	4.95 E+5	6.77 E+5
5	1.0 E-3	1.3 E-8	0	0	7E-10	1.09 E+4	1.63 E+4	2.15 E+4	2.40 E+4	3.46 E+4	4.69 E+4	2.19 E+5	3.47 E+5	4.39 E+5	6.01 E+5
6	3.7 E-4	1.7 E-3	0	0	4.7 E-8	1.38 E+4	2.06 E+4	2.72 E+4	3.03 E+4	4.36 E+4	5.92 E+4	2.77 E+5	4.38 E+5	5.54 E+5	7.59 E+5
7	4.2 E-4	1.6 E-8	0	0	1.7 E-3	1.46 E+4	2.18 E+4	2.89 E+4	3.22 E+4	4.64 E+4	6.29 E+4	2.94 E+5	4.65 E+5	5.89 E+5	8.06 E+5
8	6.0 E-4	3.8 E-6	0	0	2.0 E-3	1.39 E+4	2.08 E+4	2.75 E+4	3.07 E+4	4.42 E+4	5.99 E+4	2.81 E+5	4.44 E+5	5.61 E+5	7.68 E+5
9	0	2.0 E-3	0	0	2.0 E-8	1.45 E+4	2.17 E+4	2.87 E+4	3.20 E+4	4.61 E+4	6.25 E+4	2.93 E+5	4.63 E+5	5.85 E+5	8.02 E+5
10	3.8 E-8	0	0	0	2.1 E-3	1.33 E+4	1.99 E+4	2.63 E+4	2.93 E+4	4.22 E+4	5.73 E+4	2.68 E+5	4.24 E+5	5.36 E+5	7.34 E+5

11	0	0	0	0	1.4 E-9	1.73 E+4	2.58 E+4	3.41 E+4	3.81 E+4	5.48 E+4	7.44 E+4	3.48 E+5	5.50 E+5	6.96 E+5	9.53 E+5
12	0	0	0	0	6E-10	1.67 E+4	2.50 E+4	3.30 E+4	3.68 E+4	5.30 E+4	7.19 E+4	3.36 E+5	5.32 E+5	6.73 E+5	9.21 E+5
13	2.7 E-3	3.1 E-4	0	0	1.9 E-7	1.62 E+4	2.42 E+4	3.19 E+4	3.56 E+4	5.13 E+4	6.95 E+4	3.25 E+5	5.15 E+5	6.51 E+5	8.91 E+5
14	2.2 E-4	1.22E-3	0	0	9.6 E-5	1.48 E+4	2.22 E+4	2.93 E+4	3.27 E+4	4.71 E+4	6.38 E+4	2.99 E+5	4.72 E+5	5.97 E+5	8.18 E+5
15	0	1.0 E-7	0	0	2.4 E-3	1.52 E+4	2.27 E+4	3.00 E+4	3.34 E+4	4.82 E+4	6.53 E+4	3.06 E+5	4.83 E+5	6.12 E+5	8.37 E+5
16	1.2 E-3	0	0	0	2.7 E-4	1.40 E+4	2.09 E+4	2.76 E+4	3.08 E+4	4.43 E+4	6.01 E+4	2.81 E+5	4.45 E+5	5.62 E+5	7.70 E+5
17	2.10E-10	2.24E-7	0	0	1.2 E-3	1.59 E+4	2.38 E+4	3.15 E+4	3.51 E+4	5.05 E+4	6.85 E+4	3.21 E+5	5.07 E+5	6.41 E+5	8.78 E+5

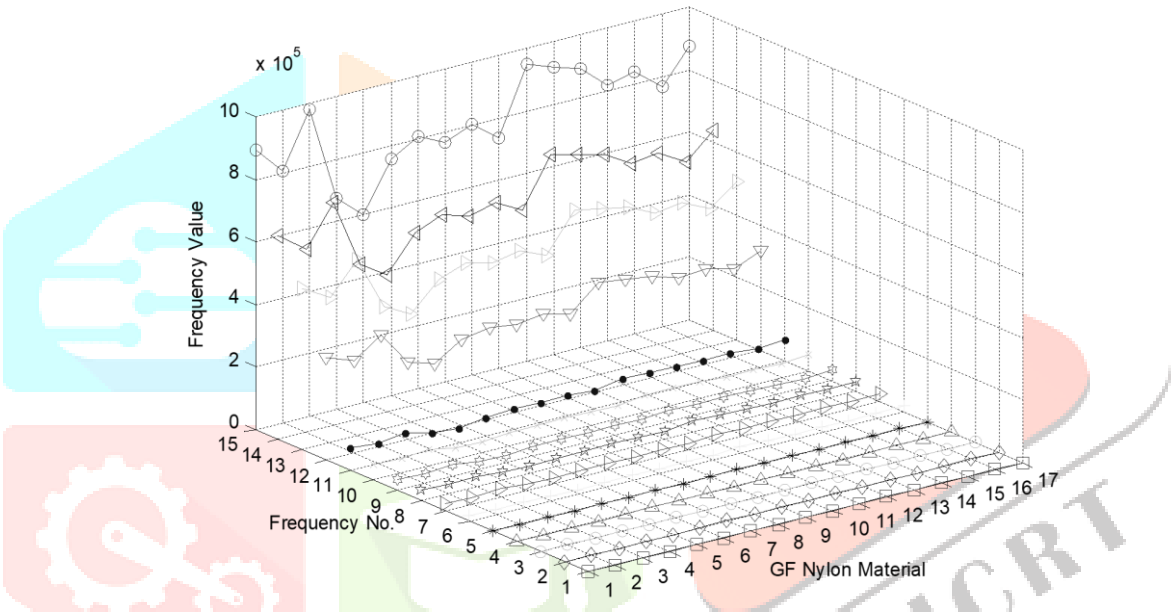

Fig. 16 Natural Frequency using Micropolar Elasticity Theory for GF Nylon Materials

From Fig. 16, it is depicted that, the natural frequency (ω_{15}) is maximum for N6-G33L 33% GFR+ (GF Mat No. 03) ω_{15} is minimum for Zytel (82G33L) (GF Mat No. 05). It can be noted that the natural frequencies obtained using MET were high when compared to those obtained from CET

The natural frequencies of different carbon filled nylon plate obtained using MET were given in Table No. 8. Comparing to the frequencies obtained for glass filled nylon plate, the frequencies of carbon filled nylon plate were very high, this was because of the fact that the strength carbon filled nylon materials were high when compared to glass filled nylon materials.

Table 8 Natural frequencies of different carbon filled nylon plate using MET

CF Mat No.	Natural Frequency (ω_n)														
	1	2	3	4	5	6	7	8	9	10	11	12	13	14	15
1	2.4 E-3	0	0	9.30 E-9	8.2 E-4	2.58 E+4	3.86 E+4	5.11 E+4	5.69 E+4	8.20 E+4	1.11 E+5	5.21 E+5	8.23 E+5	1.04 E+6	1.43 E+6
2	2.4 E-3	0	0	9.29 E-5	6.8 E-4	2.73 E+4	4.09 E+4	5.40 E+4	6.02 E+4	8.68 E+4	1.18 E+5	5.51 E+5	8.71 E+5	1.10 E+6	1.51 E+6
3	2.5 E-4	2.13 E-8	0	0	2.53 E-3	2.40 E+4	3.58 E+4	4.73 E+4	5.28 E+4	7.60 E+4	1.03 E+5	4.83 E+5	7.63 E+5	9.65 E+5	1.32 E+6
4	0	0	0	6.04 E-9	2.38 E-3	2.47 E+4	3.69 E+4	4.87 E+4	5.43 E+4	7.83 E+4	1.06 E+5	4.97 E+5	7.86 E+5	9.94 E+5	1.36 E+6
5	0	5.81 E-4	0	0	0	2.44 E+4	3.64 E+4	4.81 E+4	5.37 E+4	7.73 E+4	1.05 E+5	4.91 E+5	7.76 E+5	9.81 E+5	1.34 E+6
6	2.4 e-3	2.08 e-3	0	0	5.78 E-8	2.24 E+4	3.34 E+4	4.42 E+4	4.93 E+4	7.10 E+4	9.63 E+4	4.51 E+5	7.12 E+5	9.01 E+5	1.23 E+6
7	9.2 e-4	0	0	1.02 E-6	3.32 E-9	2.31 E+4	3.46 E+4	4.57 E+4	5.10 E+4	7.34 E+4	9.95 E+4	4.66 E+5	7.37 E+5	9.32 E+5	1.28 E+6
8	1.1 E-9	0	0	8.15 E-8	4.06 e-4	1.17 E+4	1.74 E+4	2.30 E+4	2.57 E+4	3.70 E+4	5.02 E+4	2.35 E+5	3.71 E+5	4.70 E+5	6.43 E+5
9	0	0	0	1.59 E-9	3.95 E-3	1.84 E+4	2.75 E+4	3.64 E+4	4.06 E+4	5.85 E+4	7.93 E+4	3.71 E+5	5.87 E+5	7.42 E+5	1.02 E+6

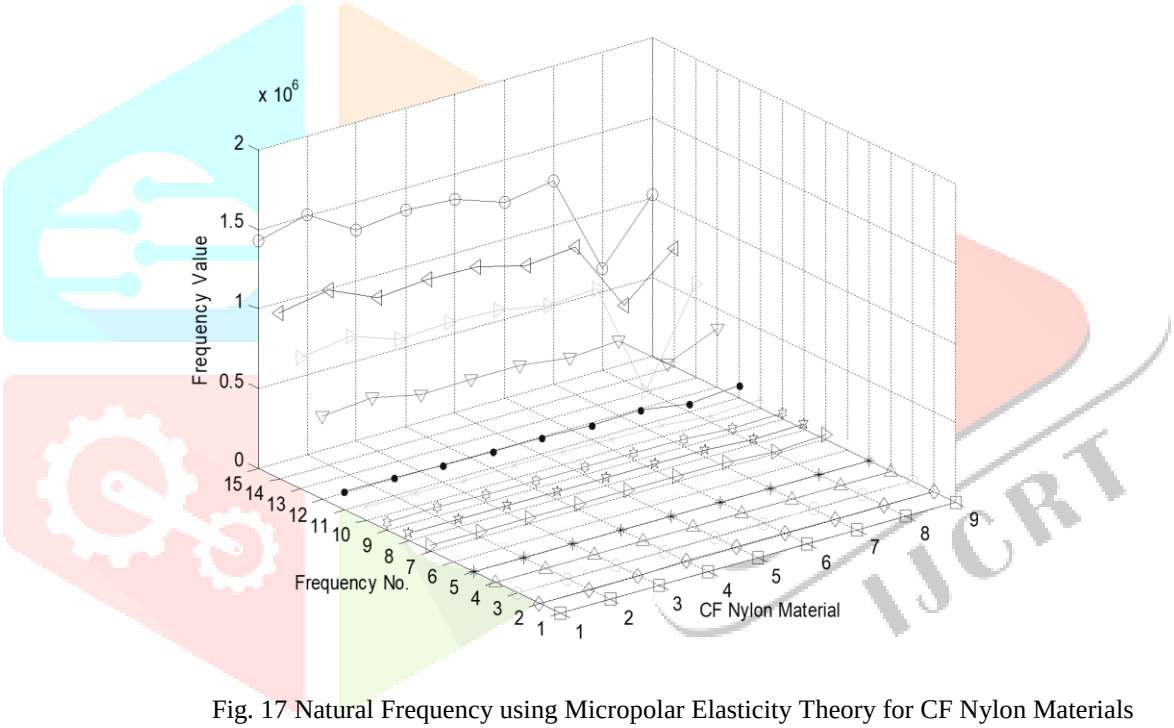

Fig. 17 Natural Frequency using Micropolar Elasticity Theory for CF Nylon Materials

As shown in Fig 17, the natural frequency (ω10) is maximum for Electrafil CF/30/TF13s12 (GF Mat No. 02)ω10 is minimum for RTP 299X51265F (GF Mat No. 08)

8. Conclusions:

In this paper, Eringen's Micropolar elasticity theory, Classical Elasticity theory, the finite element method and the 2D 3-node linear triangular element were used to develop FEM programs for analyzing a rectangular plate structure for different types of glass filled and carbon filled nylon materials which are available commercially. Some of the important results are summarized as follows:

(1) Although there is change in displacements for different types of materials, their corresponding structural Poisson's ratio for the deformed plate remains constant.

(2) It was found from the above results that the carbon filled nylon plate was having less value of strains when compared to glass filled nylon materials in the case of both MET and CET.

(3) From Fig. 4, 5, 7 and 8, which shows the variation of strains ε_{xx} and ε_{yy} for both Micropolar and classical theory depicts that for both types of nylon materials (i.e., GF and CF), the strains obtained using Micropolar theory are high than those of obtained from classical theory, this is because of considering micro-rotations.

(4) A validation check was done using ANSYS to validate strains obtained using CET shown in Fig. 10, 11, 12, 13 and it was found to have an error percentage of 0.0619.

(5) Modal analysis was done assuming as un-damped free vibration using both CET and MET and for both glass filled and carbon filled nylon plate, these results were been compared.

(6) Fig. 14 and 15 shows the natural frequencies for glass filled and carbon filled nylon plates respectively obtained using CET and Fig. 16 and 17 shows the natural frequencies for glass filled and carbon filled nylon plates obtained using MET. In both the cases,

(7) From Table 5, 6, 7 and 8 it was found that frequencies obtained using MET was high compared to CET and also found that carbon filled nylon plate was having high frequency than those of glass filled nylon plate.

9. References:

1. A. C. Eringen, "Linear theory of micropolar elasticity," J. Math. Mech. 15 (6) (1966) 909-923.
2. A. C. Eringen, E. S. Suhubi, "Nonlinear theory of simple micro-elastic solids-I", Int. J. Eng. Sci. 2 (1964) 189-203.
3. E. S. Suhubi, A. C. Eringen, "Nonlinear theory of simple micro-elastic solids-II", Int. J. Eng. Sci. 2 (1964) 389-404.
4. Y.C. Fung, "Foundation of Solid Mechanics", Prentice-Hall, Inc., Englewood Clifs, NJ, 1968.
5. R. Lakes, "Foam structures with a negative Poisson's ratio", J. Mater. Sci. 235 (1987) 1038–1040.
6. J.B. Choi, R.S. Lakes, "Non-linear properties of polymer cellular materials with a negative Poisson's ratio, J. Mater. Sci. 27 (1992) 4678–4684.
7. D.U. Yang, F.Y. Huang, "Analysis of Poisson's ratio for a micropolar elastic rectangular plate using the Finite element method", Eng. Comput. 18 (7–8) (2001) 1012–1030.
8. S. C. Cowin, "An incorrect inequality in micropolar elasticity theory", Z. Angew. Math. Phys. (J. Appl. Math. Phys.) 21 (1970) 494–497.
9. S. Nakamura, R. Benedict, R. Lakes, "Finite element method for orthotropic micropolar elasticity", Int. J. Eng. Sci. 2 (3) (1984) 319–330.
10. S. Nakamura, R. Lakes, "Finite element analysis of Saint-Venant end effects in micropolar elastic solids", Eng. Comput.12 (1995) 571–587.
11. R.D. Gauthier, W.E. Jahsman, "A quest for micropolar elastic constants", J. Appl. Mech.-T. ASME 42 (1975) 369–374.
12. R.D. Gauthier, "Analytical and experimental investigations in linear isotropic micropolar elasticity", Doctoral Dissertation, University of Colorado, 1974.
13. T. R. Chandrupatla, A. D. Belegundu, "Introduction to Finite Element in Engineering", 2nd Edition, Prentice-Hall International, Inc., Englewood Cliffs, NJ, 1997.
14. Larry J. Segerlind, "Applied Finite Element Analysis", 2nd Edition
15. Leonard Meirovitch, "Fundamentals of Vibrations", Int. Edition 2001, McGraw-Hill Companies, Inc., New York.
16. Courtesy: http://www.matweb.com/
17. Courtesy: http://www.ptsllc.com/
18. Courtesy: http://www.boedeker.com/noryl_p.htm
19. Others courtesy: Plastics Digest, Principal Properties, ed. 19, Vol. 2, 1998, D.A.T.A. Business Publishing